Ferreira, Filipe V.; Otoni, Caio G.; De France, Kevin J.; Barud, Hernane S.; Lona, Liliane M.F.; Cranston, Emily D.; Rojas, Orlando J.

Porous nanocellulose gels and foams : Breakthrough status in the development of scaffolds for tissue engineering

Published in:
Materials Today

DOI:
10.1016/j.mattod.2020.03.003

Published: 01/07/2020

Document Version
Publisher's PDF, also known as Version of record

ELSEVIER

RESEARCH: REVIEW

Porous nanocellulose gels and foams: Breakthrough status in the development of scaffolds for tissue engineering

Filipe V. Ferreira [1,2], Caio G. Otoni [2], Kevin J. De France [3], Hernane S. Barud [4], Liliane M.F. Lona [1], Emily D. Cranston [5,7,*], Orlando J. Rojas [2,5,6,7,*]

[1] School of Chemical Engineering, University of Campinas (UNICAMP), Campinas, 13083-970 São Paulo, Brazil
[2] Department of Bioproducts and Biosystems, School of Chemical Engineering, Aalto University, Espoo FI-00076, Finland
[3] Laboratory of Cellulose & Wood Materials, Empa – Swiss Federal Laboratories for Materials Science and Technology, Überlandstrasse 129, 8600 Dübendorf, Switzerland
[4] Biopolymers and Biomaterials Laboratory (BIOPOLMAT), University of Araraquara (UNIARA), Araraquara, 14801-340 São Paulo, Brazil
[5] Department of Chemical & Biological Engineering, 2360 East Mall, The University of British Columbia, Vancouver, BC V6T 1Z3, Canada
[6] Department of Chemistry, 2036 Main Mall, The University of British Columbia, Vancouver, BC V6T 1Z3, Canada
[7] Department of Wood Science, 2424 Main Mall, The University of British Columbia, Vancouver, BC V6T 1Z3, Canada

We report on the latest scientific advances related to the use of porous foams and gels prepared with cellulose nanofibrils (CNF) and nanocrystals (CNC) as well as bacterial nanocellulose (BNC) – collectively nanocelluloses – as biomedical materials for application in tissue regeneration. Interest in such applications stems from the lightweight and strong structures that can be efficiently produced from these nanocelluloses. Dried nanocellulose foams and gels, including xerogels, cryogels, and aerogels have been synthesized effortlessly using green, scalable, and cost-effective techniques. Methods to control structural features (*e.g.*, porosity, morphology, and mechanical performance) and biological interactions (*e.g.*, biocompatibility and biodegradability) are discussed in light of specific tissues of interest. The state-of-the-art in the field of nanocellulose-based scaffolds for tissue engineering is presented, covering physicochemical and biological properties relevant to these porous systems that promise groundbreaking advances. Specifically, these materials show excellent performance for *in vitro* cell culturing and *in vivo* implantation. We report on recent efforts related to BNC scaffolds used in animal and human implants, which furthermore support the viability of CNF- and CNC-based scaffolds in next-generation biomedical materials.

Keywords: Cellulose nanofibrils; Cellulose nanocrystals; Foams; Aerogels; Cryogels; Xerogels

Introduction

The search for functional biomaterials to assist with the regeneration of damaged biological tissues has recently gained extensive attention [1,2]. Grafts and metal implants that have traditionally been used for such purposes [3,4] are now being replaced by polymer-based materials, which demonstrate several favorable properties that are gained by controlling material structuring, morphology and porosity [5,6]. These emerging polymer-based biomaterials have been used as extracellular matrix (ECM) analogues or "scaffolds" to promote a variety of cellular functions, *i.e.*, cell attachment, differentiation, maturation, and matrix production [7]. Furthermore, due to the generally high level of control over scaffold porosity, cell migration beyond its surface, *e.g.*, throughout the entirety of the material, enables enhanced tissue regeneration *versus* traditional grafts and metal implants [8]. Functional scaffolds have been prepared from several synthetic

* Corresponding authors.
E-mail addresses: Cranston, E.D. (emily.cranston@ubc.ca), Rojas, O.J. (orlando.rojas@ubc.ca), Rojas, O.J. (orlando.rojas@aalto.fi).

polymers [9,10], however, the high production costs associated with complex preparation methods [11–13], and concerns regarding material biocompatibility, sustainability, and environmental impact [14,15] have prompted research into greener alternatives.

As a result, plant and other natural fibers such as those based on cellulose, chitin, and other biopolymers, have been increasingly used to prepare functional scaffolds through simple and cost-effective methods [16,17]. The term nanocellulose is used herein to refer generically to any of the main types of materials that include long, flexible cellulose nanofibrils (CNF), short, rigid cellulose nanocrystals (CNC), and highly pure, crystalline bacterial nanocellulose (BNC). They have all emerged as attractive candidates for producing dried foams and other ultra-lightweight materials including aerogels, cryogels, and xerogels – minding clear conceptual differences as discussed elsewhere [18,19]. The types of nanocellulose-based materials considered in this review as precursors for "scaffolds" generally exhibit biocompatibility [20], excellent mechanical strength [21], and highly porous three-dimensional (3D) structures with relatively high specific surface area [22,23] and hierarchical organization [24,25].

In this contribution, we provide an overview of the state-of-the-art on the rapidly growing field of nanocellulose-based scaffolds for tissue engineering. From a materials science standpoint, we build the discussion from an overview of the use of nanocellulose as a bottom-up building block to prepare structured and porous materials, and summarize the groundbreaking progress within the context of tissue engineering. Relevant structure–processing–property relationships are critically established, with an emphasis on techniques to fabricate and tailor these materials to fulfill the biological (*e.g.*, biocompatibility and cytotoxicity) and physical (*e.g.*, porosity, morphology, and mechanical integrity) requirements of tissue engineering scaffolds. Finally, the commercial prospects of nanocellulose biomaterials and our perspective on ongoing challenges within the field are discussed. We would also like to direct any interested reader to the several other published reports focused on the general preparation, characterization, and various uses of porous nanocellulose materials [18,26–30].

Nanocellulose: definitions and hierarchical assemblies

Chemically, cellulose is a linear, high molecular weight homopolymer of D-glucose repeating units linked by β-1,4-glycosidic bonds. Since Anselme Payen elucidated the natural occurrence of this macromolecule in the early 19th century [31], cellulose has been extensively investigated for a range of applications, as addressed elsewhere [32–34]. Recently, the building blocks formed during the multiscale, hierarchical assembly of cellulose, *i.e.*, nanocelluloses – mostly individualized CNF and CNC as well as BNC – have received great attention, particularly, in the present context, for their prospects in biomedical applications [35,36].

Characterized by highly ordered and non-ordered domains, CNF are one of the smallest structural units of plant fibers [37]. Generally, CNF are isolated from cellulosic fibers through mechanical defibrillation after optional chemical (*e.g.*, TEMPO-mediated oxidation, carboxymethylation, phosphorylation and others) [38] and/or enzymatic [39] pretreatments. Detailed production procedures to obtain CNF have been extensively described by Nechyporchuk et al. [40] and Abdul Khalil et al. [41]. Here, it is worth noting that different starting materials and defibrillation protocols lead to CNF with distinctly different dimensions and properties. Importantly, the use of commercial wood fibers with minimum or negligible heteropolysaccharide and lignin content, following chemical or enzymatic pretreatments, lead to CNF of high quality and purity [42], which is critical when considering them as starting materials for biomedical applications. Regardless of source and processing conditions, CNF have diameters of 5–50 nm, and lengths of up to a few micrometers, and are characterized in general by their good flexibility/elasticity and concurrent mechanical stiffness (modulus from 10 to 50 GPa) [43,44]. Because of their large aspect ratio (100 or higher), hygroscopicity, and flexibility, CNF easily form hydrogels, even at low concentrations (*ca.* 1 wt.%) [45]. Such systems are characterized by highly entangled and interconnected networks, which are advantageous for the preparation of scaffolds.

In contrast, CNC are highly crystalline rigid rod-shaped particles produced *via* chemical hydrolysis or oxidation of cellulosic fibers, which selectively removes the less ordered domains that are otherwise present in structures such as CNF [46]. Generally, the main chemical and structural features of CNF also apply to CNC, but these materials can be differentiated by their crystallinity (higher in CNC); morphology (fibrillar in CNF *versus* spindle-like in CNC); aspect ratio (typically 5–30 for CNC); mechanical behavior (CNF is flexible whereas CNC is stiff with compressive modulus of *ca.* 150 GPa); and surface chemistry, the latter of which is mostly determined by the protocol used to isolate CNC, although both materials can be readily surface-functionalized post-production [47,48]. Furthermore, given the nature of the strong acids and oxidizing agents used to produce CNC, these materials are fairly consistent across different suppliers and starting materials, have undetectable lignin/hemicellulose content, are white in color when dried, and have a higher purity than their CNF counterparts [49]. Compared to CNF, the lower aspect ratio CNC require a higher concentration to form a network/gel in water (*ca.* 10 wt.%), although this is heavily dependent on source material, surface chemistry, and ionic strength [50].

BNC, also commonly referred to as microbial cellulose or biocellulose, represents a particular class of nanocellulose that is produced from low-molecular weight carbon sources by Gram-negative acetic acid bacteria (*e.g.*, *Komagataeibacter xylinus*). Like CNF and CNC, BNC is renewable and biocompatible, but is characterized by a higher crystallinity and purity – *i.e.*, compared to its plant-derived analogues, BNC is completely devoid of lignin and hemicellulose [51,52] and, as a result, it has enjoyed a broader interest throughout the biomedical community. BNC is charge-neutral and is produced as a hydrogel-like biofilm that is thermally and mechanically stable despite having a relatively low solids content (*ca.* 0.5–2 wt.%) [52]. BNC can also be further processed into individualized nano-ribbons or chemically treated to produce BNC-derived CNC that tend to be more crystalline and have a larger aspect ratio compared to their plant-based counterparts [53].

Considering the relatively low manufacturing costs of nanocelluloses (estimated to range from US$ 1375 to 1630/t for cellulose micro/nanofibrils [54] and from US$ 3632 to 4420/t for CNC [55]) and the vast spectrum of material properties achievable with different types of nanocellulose-based materials, potential applications include – but are not limited to – printed electronics [56], polymer nanocomposites [57], papermaking [58], water purification [59,60], energy storage devices [61], and food packaging [62]. Recently, the intrinsic properties of cellulose at the nanoscale have been exploited for the development of low-density structures displaying high porosity and surface area, namely gels and foams [57,63]. These porous materials can be used either in a hydrated state, filled with water or other compatible solvents, or in a dried form, filled with air [64]. Porous materials such as these are potential candidates for a wide range of applications, including shock-absorbing materials [65], drug delivery systems [66,67], thermal and acoustic insulators [68], (super)absorbents [65,69], environmental remediators [70], and scaffolds for biomedical applications [71]. Each of these applications has specific technical requirements, necessitating the customization of material properties and characteristics, highlighting the versatility of nanocellulose-based materials.

Note that regardless of preparation technique, scaffolds need to be wet-resilient for applications in tissue engineering; this is because of the prevailing hydrated *in vivo* environment. Ultimately, any scaffold will become wet/rewetted in the body, even if it was initially dried, and therefore, will eventually become a hydrogel. An extensive number of reports are available covering the use of nanocellulose hydrogels for tissue engineering [26]; however, in the context of the present discussion we assumed that the initial state of the scaffold is in the dried form, which facilitates better tailoring of the properties of the system to the given demands.

Nanocellulose assembly into scaffolds

Current biomaterials used for scaffold fabrication include metals, ceramics, and polymers, as well as combinations of these materials. From the mechanical performance standpoint, difficulties in controlling the residual stress of metals and the inherent brittleness of ceramics are disadvantages that are not observed in most polymer-based scaffolds, including nanocellulose. Taking into account the high specific surface area of both nanocelluloses and porous scaffolds, an additional energy-absorbing mechanism that contributes to energy dissipation throughout the prepared scaffold gives rise to improved mechanical performance. From a processing standpoint, the facile, green, inexpensive, and scalable approach to achieving lightweight, strong, and highly interconnected 3D nanocellulose-based scaffolds brings many advantages over the current strategies for fabricating scaffolds based on metals, ceramics, and other polymers, many of which involve solvents, multi-steps, and high manufacturing costs [72–74]. Moreover, nanocellulose materials can be processed into virtually any desired shape, which may not be as straightforward for metal and ceramic materials, for example.

The overall design and properties of porous materials are highly dependent on the preparation strategy used, which in general involves two main steps: the preparation of a suspension or gelled network, and the creation of pores *via* structuring and/or solvent removal. In the case of nanocellulose-based scaffolds, there are several strategies that have traditionally been used for this purpose, and can broadly be classified into three groups: porogen templating, sacrificial templating, and extrusion (Fig. 1). Furthermore, in addition to the preparation strategy used, the properties of the starting nanocellulose material greatly influence the resulting scaffold properties. The following sections discuss the design considerations associated with the creation of nanocellulose-based scaffolds, broken down by methodology.

Porogen templating

Traditionally, porogen templating utilizes the generation of gas bubbles (through high-intensity stirring or air sparging) within an aqueous dispersion [75] followed by gelation/curing of the continuous phase, with possible intermediate steps involving solvent exchange [18], and subsequent oven drying. Typically, porogen templating results in nanocellulose 'foams' (average pore sizes *ca.* 200 μm). Although this process is simple and scalable when compared to traditional mineral and polymer sol–gel processes [76], the size and shape of the formed pores is limited due to a relative lack of control over the morphology of the gas bubbles generated. Furthermore, care needs to be taken to avoid coalescence/partitioning of the inherently unstable gas bubbles during scaffold formation/drying, which can lead to scaffolds with compromised mechanical stability. However, due to the anisotropic nature of nanocellulose, coalescence can be somewhat minimized *versus* suspensions of isotropic particles, given the high surface coverage and entanglement of nanocellulose [77]. Because of this, the longer and more entangled CNF are used with much more prevalence than their shorter CNC counterparts. Other variables that affect pore formation include shear forces during mixing [78] and fibril flexibility [79], whereby smaller pores are expected by using higher shear and more flexible fibrils. Compared to foams prepared by quenching CNF suspensions in temperature-controlled baths, foams prepared by mechanical stirring and quenching have been demonstrated with bimodal pore sizes and improved mechanical properties [80].

Mariano et al. [81] correlated the porous structure and mechanical properties of CNF-based dried foams with the degree of CNF agglomeration in the precursor suspension. It was shown that the addition of cationic surfactants led to more packed CNF domains and resulted in foams with thicker walls (blue regions in μCT reconstructions shown in Fig. 2b). The authors also went on to demonstrate that the longer the hydrophobic tail ($_X$) of the C_XTAB surfactant used, the thicker the walls of the resulting CNF foam. On the other hand, the best mechanical properties were found for foams featuring a homogeneous structure, created by the association of CNF and C_{12}TAB. Similar results were found by other authors [82] by adding a non-ionic surfactant to prepare foams with improved strength *versus* CNF-only foams.

Li et al. [83] observed that relatively longer CNF exhibit weakened inter-fibril hydrogen bonding in relation to shorter CNF, which resulted in scaffolds lacking pore uniformity and decreased internal bonding strength. The simple procedure reported by the authors to control the structure and properties

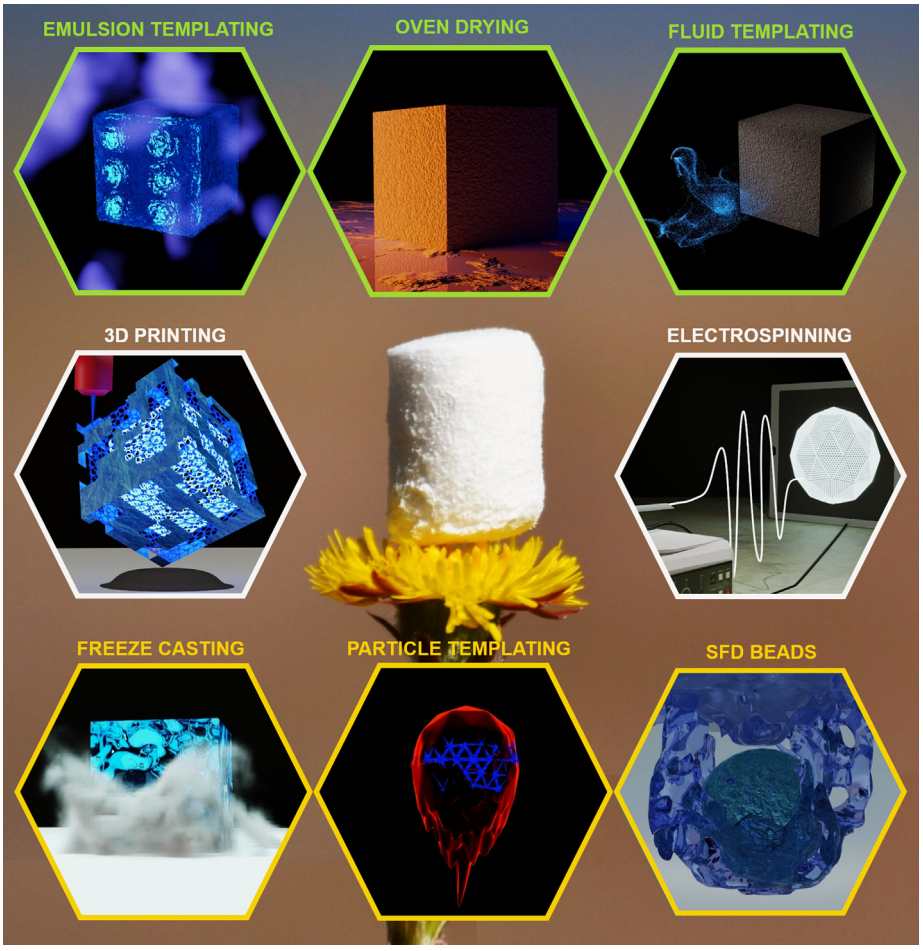

FIGURE 1

Strategies to produce nanocellulose-based scaffolds that have traditionally been used for tissue engineering. The methods are classified into three groups: green (top) – porogen templating; white (middle) – extrusion; yellow (bottom) – sacrificial templating.

of dried foams, while varying the binding and size of the fibrils through the degree of fibrillation, led to a material that combined high porosity, uniform pore size distribution, and improved mechanical properties. Kriechbaum et al. [84] also showed that the compressive strength and porous morphology of CNF foams are related to the degree of nanofibrillation. As such, a porogen templating approach with air bubbles is a robust strategy to produce porous nanocellulose structures where the starting nanocellulose physical properties strongly affect the resulting materials.

Sacrificial templating

Sacrificial templating is the most widely used method for creating nanocellulose-based porous materials, due to the range of preparation techniques falling within this category, and the range of pore sizes/morphologies achievable through this method. This technique involves the creation of a template within a nanocellulose suspension or gel, which can then be manipulated to form various pore morphologies, and is then subsequently removed through various means. In general, sacrificial templating requires that the material used as a scaffold matrix (nanocellulose), and the solid/liquid sacrificial template, form distinct phases and that their physicochemical properties are different enough to allow template removal by either physical, thermal, or chemical means.

Typically, a solvent such as water is used in sacrificial templating, however care needs to be taken to prevent pore collapse upon its removal. As such, either supercritical or freeze–drying are commonly used to ensure pore stabilization within the final porous materials. In fact, material shrinkage, density, porosity, specific surface area, and pore size, size distribution, and interconnectivity are remarkably dependent on the drying technique used: supercritical drying usually leads to smaller pores (typically micro and mesopores) [85] *versus* freeze–drying, which in turn leads to macroporous analogues [64]. Note that many examples in the literature use a freezing step (sometimes combined with solvent exchange) prior to supercritical drying to induce a networked structure. Nevertheless, should high specific surface area be targeted, water as suspending medium can be replaced by *tert*-butanol prior to freeze–drying [86]. The combined process of ice-templating and freeze–drying is herein named freeze–casting. But such combination is not a requirement, for example, in already structured/entangled CNF systems, direct supercritical drying to form aerogels is possible [87] but in dilute CNC suspensions, supercritical drying without freezing leads to materials that do not hold together when dried [65,88].

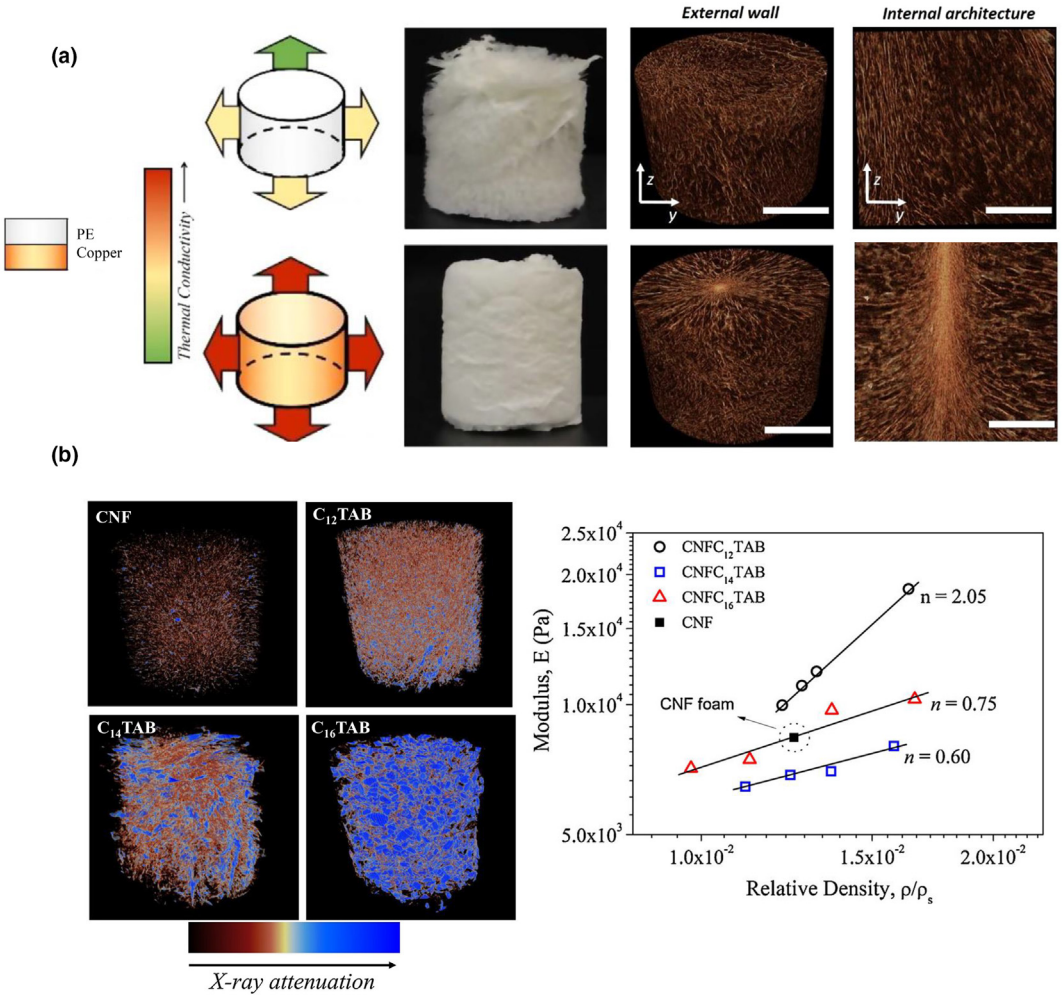

FIGURE 2

(a) Thermal conductivity (left) of copper (top) and polyethylene (bottom) molds used for freezing CNF suspensions prior to freeze–drying into CNF dried foams (center; digital images) with different microstructures (right; X-ray micro-computed tomography (μCT) reconstructions; scale bar = 5 mm). (b) μCT reconstructions of neat CNF foams and CNF-based foams prepared by using cationic surfactants (C_{12}TAB, C_{14}TAB, and C_{16}TAB), and their mechanical behavior. Adapted from (a) Ref. [108], (b) Ref. [81] with the permission of Elsevier.

Freeze–casting relies on the low solubility of cellulose in most liquids, which allows the physically-induced separation of cellulose during the crystallization of the suspending medium [89]. The process consists of freezing the liquid (usually water) followed by sublimation of the frozen phase [80,90], yielding a dry, highly interconnected 3D network where voids or pores replace the formerly present crystals [89,91], *i.e.*, ice-templated structures or cryogels. Ice sublimation prevents formation of a liquid/vapor interface and avoids the collapse of the 3D nanocellulose structure [18]. Depending on the details of the freeze-casting process, materials featuring different properties can be obtained [92,93]. For instance to control the discrete structure of the scaffolds, Cai et al. [94] prepared cross-linked CNF cryogel microspheres, ranging from 60 to 120 μm in diameter, by spraying and atomizing CNF aqueous gels directly into liquid nitrogen prior to freeze–drying. Other methods have been proposed to produce porous nanocellulose beads, including spray freeze–drying (SFD) [95], droplet templating *via* microfluidics followed by evaporative or freeze–drying [96], reductive amination of dialdehyde cellulose followed by solvent exchange and evaporative drying [97], and droplet casting onto a superhydrophobic surface followed by freeze–thawing, solvent exchange, and evaporative drying [98].

As stated above, freeze–drying involves turning ice crystals into pores, which takes place along the direction of the solidification front [99]. In this sense, the internal morphology of nanocellulose scaffolds can be tailored by controlling the crystallization of the precursor suspensions. Homogeneous and unidirectional freezing steps have been demonstrated to lead to nanocellulose foams with 3D cellular and honeycomb structures, respectively [100]. Chau et al. [101] produced scaffolds with fibrillar, columnar, or lamellar morphologies by varying the CNC/poly(oligoethylene glycol methacrylate) ratio and the freeze–casting temperature. The produced materials presented anisotropic swelling and mechanical behaviors suitable as biomimetic scaffolds for the regeneration of oriented tissues. Additionally, the size of the pores usually decreases as the solidification rate increases [102]; a slow freezing can lead to segregation between the continuous and the dispersed phases, offering another level of control [89].

The internal porous structure of dried gels and foams is strongly connected with their macroscopic properties. Sehaqui et al. [64] tailored the porosity of freeze-cast CNF foams from 93.1 to 99.5% by using different CNF contents in the precursor suspensions (0.7–10 wt.%) and tuned the foam's compressive modulus and yield strength from 56 kPa to 5.3 MPa and from 7.8 to 516 kPa, respectively. In this sense, ice-templating is a suitable way to form scaffold microstructures and to gain control on their properties [103–106]. Chen et al. [107] prepared chemically cross-linked anisotropic honeycomb-like carboxymethyl cellulose (CMC)/CNF cryogels through directional freeze–casting by allowing heat exchange with a dry ice-acetone solution at −78 °C only through the bottom on the pre-filled mold and reported good mechanical strength both in the directions parallel (compressive modulus up to 10 MPa) and perpendicular (flexural modulus up to 54 MPa) to the freezing direction.

Mariano et al. [108] showed that the heat conductivity of the mold used in the freezing step of freeze–casting affects the nucleation and growth of ice crystals (*e.g.*, copper is less insulating than polyethylene so freezing is faster), which in turn leads to CNF cryogels with different orientations, pore sizes, wall thicknesses, and mechanical strength (Fig. 2a). Similarly, Otoni et al. [109] tailored the porosity and pore size of cationic CNF foams by controlling the kinetics of ice crystallization, using slower freezing at milder conditions (−10 °C using polypropylene molds), and allowing ice crystals to grow to a larger extent when compared to faster freezing (at −196 °C in liquid nitrogen and using copper molds). It should be noted that rapid freezing may inflict macroscopic cracking as a side effect, however this can be prevented by a pre-cooling step at 4 °C before freezing [64]. Finally, liquefied gases other than nitrogen (*e.g.*, ethane and propane) should be considered as freezing media when extremely high freezing rates are desired, as the absence of Leidenfrost effect, commonly observed for liquid nitrogen, might lead to low or even no crystallization of water [110].

A variant of supercritical drying called pressurized gas expansion technology has recently been demonstrated to scale up nanocellulose scaffold fabrication where no ice-templating or "pre-solvent exchange" steps are required [88]. In this method, the liquid phase in a preformed CNC gel becomes the pores in the dried structure without any compacting of the nanocellulose structure. This is achieved by *in situ* solvent exchange steps (first to ethanol and then increasing the supercritical CO_2 concentration in ethanol, up to 100%) using a co-axial nozzle into a pressurized vessel, followed by depressurization and CO_2 recovery. The CNC aerogels produced were more "mound-like" and fibrillar than ice-templated aerogels and were primarily composed of mesopores and small macropores (1–4 μm), leading to high specific surface area (320 m^2/g) [88].

Interestingly, Torres-Rendon et al. [111] prepared solid methacrylate/ methacrylamide-based resin sacrificial templates *via* lithographic 3D printing; a CNF dispersion was then infiltrated throughout the template *via* centrifugation prior to template dissolution in alkaline media. The resulting CNF scaffolds had a dual porous structure; large macropores (*ca.* 1 mm from the sacrificial template) and small macropores (*ca.* 1 μm from the CNF themselves). Although solid templating such as this has rarely been used to create nanocellulose scaffolds, it allows for the possibility to create highly organized porous structures, which are not readily achievable using other methods of sacrificial templating, as those discussed here. Finally, it should be mentioned that nanocellulose itself has been used extensively as a sacrificial templating agent for the preparation of mesoporous glass, ceramics, resins, polymer hydrogels, other nanoparticles, carbonized structures, and freestanding tubular cell constructs where the cellulose is removed by calcination [112,113] or hydrolyzed by cellulases [114]. Should nanocellulose serve as a matrix for scaffold formation, examples of sacrificial templating agents include those removed by melting (agarose microparticles [115]) or leaching after solubilization in various solvent. For example, templates soluble in water (gelatin microspheres [116], sodium chloride crystals [117], poly(ethylene glycol) [118]), aqueous sodium hydroxide (silicon dioxide particles [119], lithographically printed liquid photopolymerizable resin–reverse templating [111]), acetone/chloroform (polymethylmethacrylate particles [120,121]), and tetrahydrofuran or surfactants (paraffin wax microspheres) [120,122]) have been demonstrated.

Extrusion

Extrusion-based techniques including 3D printing and electrospinning enable the production of scaffolds with controllable architectures and voids [123,124]. Typically, scaffolds produced through these methods contain interconnected macropores, which is beneficial for allowing nutrient diffusion throughout the gel network. Typically, nanocellulose is used in formulations to vary scaffold properties such as mechanical strength, swelling, and protein/cell adhesion. Electrospinning uses high voltages to stretch extruded polymer solutions into nanofibers, and has attracted interest across several fields due to its simplicity and ability to create high surface area porous "non-wovens" as scaffolds. Notably, the parameters of the electrospinning process (such as field strength, nozzle design, and flow rate) and the polymer solution (such as concentration, viscosity, and molecular weight) can be readily adjusted to alter the final structure of the scaffolds [125].

Hivechi et al. [126] demonstrated that the modulus of gelatin–CNC composite electrospun scaffolds could be enhanced by increasing the CNC loading up to 5 wt.%; however, at higher CNC loadings, the modulus decreased again attributed to CNC aggregation within the nanofibers. Several research groups have demonstrated the ability to tune the resulting fiber diameters by incorporating increasing amounts of either CNF [127,128] or CNC [129]. Varying the process parameters such as the nozzle design and collection method facilitates control on the morphology of electrospun nanocellulose scaffolds. Chao et al. [130] demonstrated the production of electrospun scaffolds with core–shell morphologies by using a coaxial nozzle. Finally, both He et al. [131] and Huan et al. [132] used rotating drum collectors to prepare electrospun scaffolds with aligned nanofibers and anisotropic properties.

3D printing uses a viscoelastic ink that is either cross-linked *in situ* or post-extrusion in order to form fibers with suitable shape fidelity. Nanocellulose is most commonly used in 3D printing as a rheology modifier in order to increase the viscosity or shear-thinning potential of an ink [133–136]. It has been

shown that increasing the concentration of CNC within "bioink" formulations leads to 3D printed scaffolds with enhanced modulus [137]; however the opposite trend is observed upon increasing CNF concentration [138,139]. Notably, Wang et al. [140] functionalized CNC with a bis(acyl)phosphane oxide photoinitiator, rendering the CNC capable of initiating the polymerization of monofunctional PEG *in situ* during 3D printing; the scaffolds 3D printed *via* this method demonstrated a high capacity for swelling *versus* uncross-linked scaffolds prepared with unmodified CNC. In sum, extrusion-based techniques such as 3D printing and electrospinning, can be combined with nanocellulose in order to create stable and biomimetic scaffolds for tissue engineering.

Biological and structural requirements for an ideal scaffold for tissue engineering

The preparation of scaffolds from natural macromolecules intended for tissue engineering has grown rapidly [57,141]. An overall strategy is to seed the patient's own cells within the scaffold before implantation in the body [142]. Scaffolds can also be used without previous cell seeding, by direct implantation to promote *in situ* cell growth, proliferation, and tissue regeneration [143]. Regardless of the approach taken, the scaffolds themselves are of critical importance since they affect cell growth and promote tissue maturation [142,144].

Recently, much research in this interdisciplinary field has focused on the development of suitable scaffolds [123,145–148]. In general, to be considered proper for tissue engineering applications, biomaterial scaffolds should meet several basic requirements, including (i) biocompatibility (related to its specific intended use), (ii) biodegradability (related to its eventual clearance *via* normal pathways), and (iii) porosity (related to effective cell/nutrient transport). In addition, scaffolds should demonstrate both (iv) similar mechanical performance, and (v) structural morphology to a tissue of interest, in order to better mimic native *in vivo* microenvironments (both tissue architecture and biological composition) [149,150]. Different properties are required depending on the tissue of interest, as shown in Fig. 3. Each of these requirements is discussed below, emphasizing the current status of nanocellulose-based scaffolds for addressing these needs.

Biocompatibility

Scaffold biocompatibility is fundamentally important for tissue engineering; this encompasses both proper function and minimal toxicity during the intended use [51,171]. Although several *in vitro* and *in vivo* studies have demonstrated that nanocellulose-based materials are non- or minimally cytotoxic [172,173,182–190,174–181], biocompatibility testing for specific applications is still largely missing. Furthermore, material

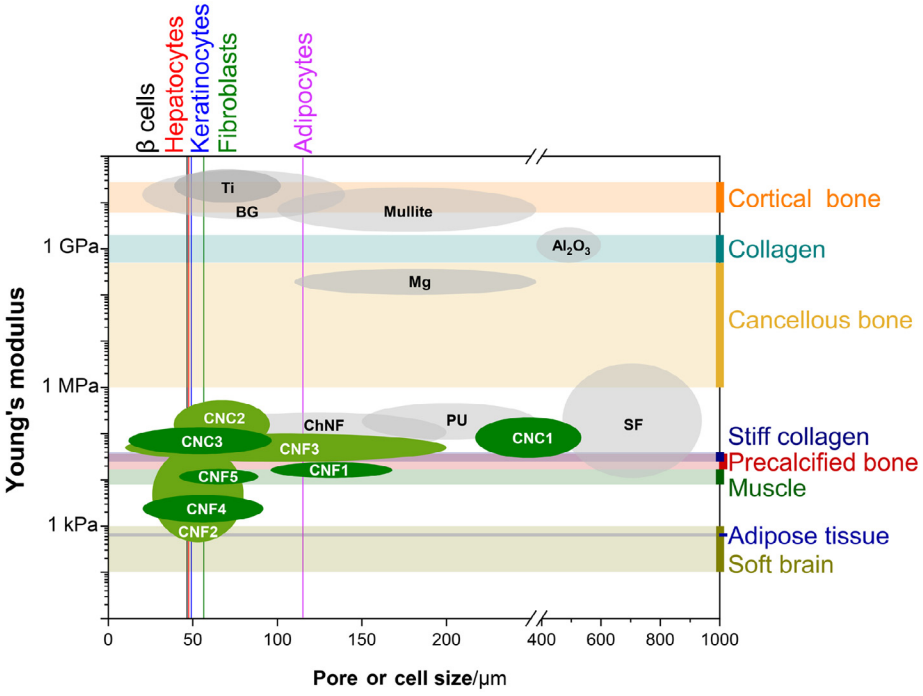

FIGURE 3

Ashby plot showing moduli and pore sizes for a variety of porous nanocellulose scaffolds in the dry state (green ovals) relative to the size of different human cell types (indicated at the top of the plot) [151] and typical compressive moduli of different human tissues (on the right) [152–157]. Grey ovals indicate other classes of porous materials envisaged for the same purpose. CNF1: CNF/bioactive glass aerogel scaffolds [158]; CNF2: cross-linked unidirectional cationic CNF cryogel scaffolds [71]; CNF3: oxidized CNF cryogel scaffolds [159]; CNF4: CNF-only cryogel scaffolds shaped in molds of varying heat conductivities [108]; CNF5: CNF/cationic surfactant cryogel scaffold [81]; CNC1: unidirectional CNC/hydroxyapatite cryogel scaffolds [160]; CNC2: poly(vinyl alcohol)-bound CNC cryogel scaffolds [161]; CNC3: tunicate CNC cryogel scaffolds [162]; ChNF: Pickering foam-templated chitin nanofibril xerogel scaffolds [163]; NaCl-templated silk fibroin cryogel scaffolds [164]; PU: polyurethanes based on 50/50 ε-caprolactone/L-lactide [165]; BG: sacrificial polymer-templated ceramic (sintered 70% SiO_2–30% CaO glass powder) scaffolds [166]; Mullite: ceramic foams [167]; Al_2O_3: alumina foams [168]; Mg: magnesium scaffolds produced through fiber deposition hot pressing [169]; Ti: unidirectional titanium foams [170].

biocompatibility is highly dependent on the route of internalization, with inhalation representing one of the major concerns due to the high aspect ratio of nanocelluloses [20,189–191]. However, implanted/injected nanocellulose-based materials are generally considered both hemocompatible and biocompatible [20,173,187,192], suggesting that these materials hold promise for tissue engineering. Finally, as there is no mechanism for the enzymatic breakdown of cellulose in humans, additional testing is needed to determine both nanocellulose's biodistribution and eventual clearance [173,179].

Biodegradability

The lack of enzymatic breakdown of nanocellulose in most species *in vivo* is an important consideration for tissue engineering. In this context, chronic toxicity studies *in vivo* should be performed to identify possible inflammatory response to nanocellulose for extended time [193]. Biomaterial scaffolds should ideally degrade *in vivo* after the formation/regeneration of new tissue [194]. This process should happen at given times, depending on the growth of the tissue of interest; as a result, it is crucial to further investigate the clearance mechanisms of nanocellulose, which do not fully biodegrade [195]. Clearance mechanisms will vary depending on the properties of the nanocellulose used (*e.g.*, type, aspect ratio, and surface chemistry). Additionally, the combination of nanocellulose with other polymeric matrices that are known to degrade, or cross-linking chemistries that have been tested *in vivo*, could affect the overall clearance of the scaffold [196,197].

Interestingly, Entcheva et al. [17] combined cellulose scaffolds with a cytocompatible enzymatic cocktail comprising endoglucanases, exoglucanases or cellobiohydrolases, and β-glucosidases, which selectively hydrolyzed cellulose into low-molecular weight building blocks that were readily biodegraded at physiological conditions. Hence, it is possible to benefit from the exclusive structural, adhesion, and shaping capabilities of nanocellulose to provide a suitable environment for *in vitro* culturing cardiac cells and growing cardiac tissue, and to simultaneously achieve the required *in vivo* biodegradability of the scaffolds to prevent any inflammatory response [17].

Porosity

Porosity, by definition, is a numerical translation of the amount of empty space in relation to the volume of a given geometry. Whereas porosity is the most remarkable characteristic that distinguishes scaffolds within the tissue engineering context, the possibility of tailoring porous 3D architectures in a straightforward fashion while maintaining structural integrity, is what makes nanocellulose particularly relevant for such a purpose. Not only are the pores themselves important, but also their interconnectivity, as this allows for the diffusion of nutrients/oxygen and waste removal [198]. Also critical is the infiltration of cells and blood vessels, which proliferate throughout the scaffold as a whole without compromising the formation of new tissues [199,200].

Nasiri et al. [201] observed that scaffolds with hierarchical morphologies combined with high porosity promote early-stage osteoinduction. In addition to porosity, cell behavior and growth of new blood vessels (angiogenesis) are also influenced by pore size, which should be controlled in order to favor tissue regeneration [148]. Murphy et al. [202] investigated the effect of scaffold mean pore size (ranging from 85 to 325 μm) on osteoblast adhesion and proliferation. They observed that the number of cells was higher in scaffolds with pores ranging from 120 to 325 μm. Mandal and Kundu [203] observed good proliferation and migration of human dermal fibroblast cells on 3D scaffolds with pore sizes of 200–250 μm. Oliviero et al. [204] reported that 30–40 μm is the minimum pore size threshold that is required for nutrient diffusion within scaffolds through blood vessels. Artel et al. [205] showed that the rate of scaffold vascularization increases with pore size and that pores ranging in size from 160 to 270 μm facilitate neovascularization. As indicated above, and as far as the application of scaffolds in tissue engineering, achieving pores within this micrometric/sub-millimetric range is the main reason why cryogels (ice-templated scaffolds) are preferred over aerogels. In this sense, ice-templating has been presented as an efficient means for fine-tuning scaffold porosity, pore size, and pore interconnectivity, although supercritically dried gels and foams (without freezing steps) are relevant for a range of applications other than tissue engineering, such as insulation, cargo delivery, catalysis, separation, and adsorption [76,85,206].

Mechanical performance

So far it is clear that porosity is essential for a range of applications involving nanocellulose 3D scaffolds; however, an increased porosity typically compromises other important properties such as mechanical strength [147]. A balance has to be achieved since scaffolds should feature a suitable mechanical performance, mimicking a native tissue microenvironment, and thus facilitating the proper migration of cells and tissue regeneration [207]. In general, nanocellulose scaffolds are capable of achieving high porosity, but the mechanical stability may not be sufficient for the engineering of stiffer tissues such as cartilage and bone, at least in load-bearing locations (Fig. 3). Therefore, covalent cross-linking of nanocellulose may be necessary to improve the mechanical properties of scaffolds while maintaining high porosity [94,208]. Among suitable cross-linkers, tannic acid [209], 1,2,3,4-butanetetracarboxylic acid (BTCA) [107,210], citric acid [211], sodium (meta)periodate [212], and commercial products such as Kymene™ [213] have been demonstrated. Depending on the chemical nature of the involved species, glyoxal [71], genipin [214], and glutaraldehyde [215] have also been reported. In addition, the formation of reversible, noncovalent cross-links such as hydrazone bonds [65,101,216–219] and supramolecular/supracolloidal interactions, including ionic cross-linking between oppositely charged nanocelluloses [26], is highly beneficial in increasing mechanical stability while simultaneously providing a mechanism for biodegradation. Finally, as the mechanical properties of nanocellulose dried gels and foams have been extensively correlated with the internal microstructure, this feature denotes another means of tailoring the performance of such materials. This association was nicely exemplified by Tripathi et al. [21], who correlated the long-range ordering of CNC into nematic and chiral nematic phases – through non-solvent induced phase separation and evaporation-induced self-assembly followed by supercritical dry-

TABLE 1

Properties of nanocellulose-based scaffolds demonstrated as suitable for tissue engineering applications through *in vitro* and/or *in vivo* testing.

Scaffold matrix	Production method[a]	Pore/channel size/μm[b]	*In vitro* assayed cells	*In vivo* model	Proposed application	Ref.
CNF	Freeze-casting	–	3 T3 NIH	–	Tissue engineering	[94]
CNF	Freeze-casting	26–80	MG-63		Bone tissue engineering	[71]
CNF	Freeze-casting	10–200	HeLa and Jurkat	–	Tissue engineering	[159]
CNF	Dissolution in ionic liquids followed by hot pressing	–	HLC and HEC	–	Tissue engineering	[252]
CNF/PVA	Freeze-casting	90 and 20	Fibroblast cells	–	Skin tissue engineering	[256]
CNF/collagen	Freeze-casting	–	Fibroblast cells	–	Tissue engineering	[24]
CNF/bioactive glass	Freeze-casting	96–168	MC3T3-E1	Calvarial bone defect in rats	Bone tissue engineering	[158]
CNF/gelatin/chitosan	Freeze-casting	75–200	ASCs and L929 cells	–	Cartilage tissue engineering	[254]
Bioactive glass coated by sulfuric acid-hydrolyzed CNC	Foam replication and dip coating	200–550	MG-63	–	Bone tissue engineering	[226]
Sodium alginate/gelatin/CNC	Oven drying	104–210	3 T3 NIH	Wound defect in rats	Skin tissue engineering	[257]
Sulfuric or phosphoric acid-hydrolyzed CNC	Critical point drying	6–11 nm and 100+ μm	Saos-2	Calvarial bone defect in rats	Bone tissue engineering	[217]
CNC/PLA	Thermally induced phase separation		Chondrocytes	–	Cartilaginous tissue engineering	[192]

[a] Freeze–casting means ice-templating plus freeze–drying. Foam replication is a method used to prepare ceramic scaffolds with high porosity, as detailed elsewhere [227,228].
[b] Average pore sizes are reported in μm unless otherwise stated.

ing after solvent exchange from water to acetone – with the mechanical strength and toughness of CNC-only aerogels.

Structural morphology

The structural characteristics of a scaffold, both at the surface and internally, play an important role for several factors, including protein adsorption and cell adhesion, which are critical in promoting natural cellular functions [220]. For example, Pattison et al. [221] observed a positive correlation between scaffold roughness and cell attachment and proliferation. Furthermore, there is additional research suggesting that smooth surfaces stimulate differentiation of multipotent cells into a specific cell type (*e.g.*, fibroblastic), while rough surfaces stimulate differentiation of other cells, such as those implicated in bone formation [222,223]. Factors such as scaffold anisotropy can also have significant effects on cell growth. For example, myoblast cells have been shown to preferentially grow in the direction of nanocellulose alignment [218,224,225]. Thus, the surface of the scaffold should be tailored according to the desired application. Overall, nanocellulose-based scaffolds should be able to attach and support tissues by offering a structurally appropriate environment for regeneration.

Tissue engineering applications of nanocellulose scaffolds

The adhesion of cells is an important first step to a scaffold's success in tissue repair or native tissue replacement. A number of preliminary works focusing on cell adhesion showed promising results in this regard. In Table 1 we summarize nanocellulose scaffolds that have been developed for specific tissue engineering applications and have reported *in vitro* and/or *in vivo* compatibility. Cai et al. [94] seeded CNF-based microspheres obtained by freeze–casting (Fig. 4a) with 3T3 NIH cell culture (embryonic fibroblast cells) and observed that the highly porous structure facilitated cell functions and allowed proper transfer of nutrients, oxygen, and metabolic wastes. Lu et al. [24] prepared CNF-based scaffolds containing collagen and achieved suitable biocompatibility and levels of cell activity and proliferation (mouse fibroblast cell; l929) for biological wound dressings.

Liu et al. [159] studied *in vitro* cell functions on CNF-based scaffolds using epithelial-derived (HeLa) and hematopoietic-derived (Jurkat) cells and reported positive outcomes concerning cell growth, survival, and proliferation, making these scaffolds promising candidates for tissue engineering applications. Courtenay et al. [71] prepared CNF-based scaffolds by directional freeze–casting (Fig. 4b) and observed that the enhanced Young's modulus, attributed to the use of glyoxal as a cross-linker, allowed for culturing osteoblast-line MG-63 cells. Li et al. [226] prepared a foam using bioactive glass dip-coated with CNC (Fig. 4c). First, the bioactive glass-based scaffolds were prepared by foam replication method, which uses polymers with the desired pore structure as a sacrificial template for the ceramic coating [227,228], and then scaffolds were coated with CNC. The authors showed that the MG-63 cells successfully attached and grew on the surface of the highly porous scaffold (Fig. 4d).

Detailed discussion on cell adhesion onto scaffolds through attachment and detachment events was reported by Khalili and Ahmad [229]. The cell adhesion can be divided into three stages (Fig. 4e–i), namely: (I) cell sedimentation; (II) cell attachment onto scaffold by integrin binding; and (III) cell spreading. Adherence is required for cells to perform their functions and to prolif-

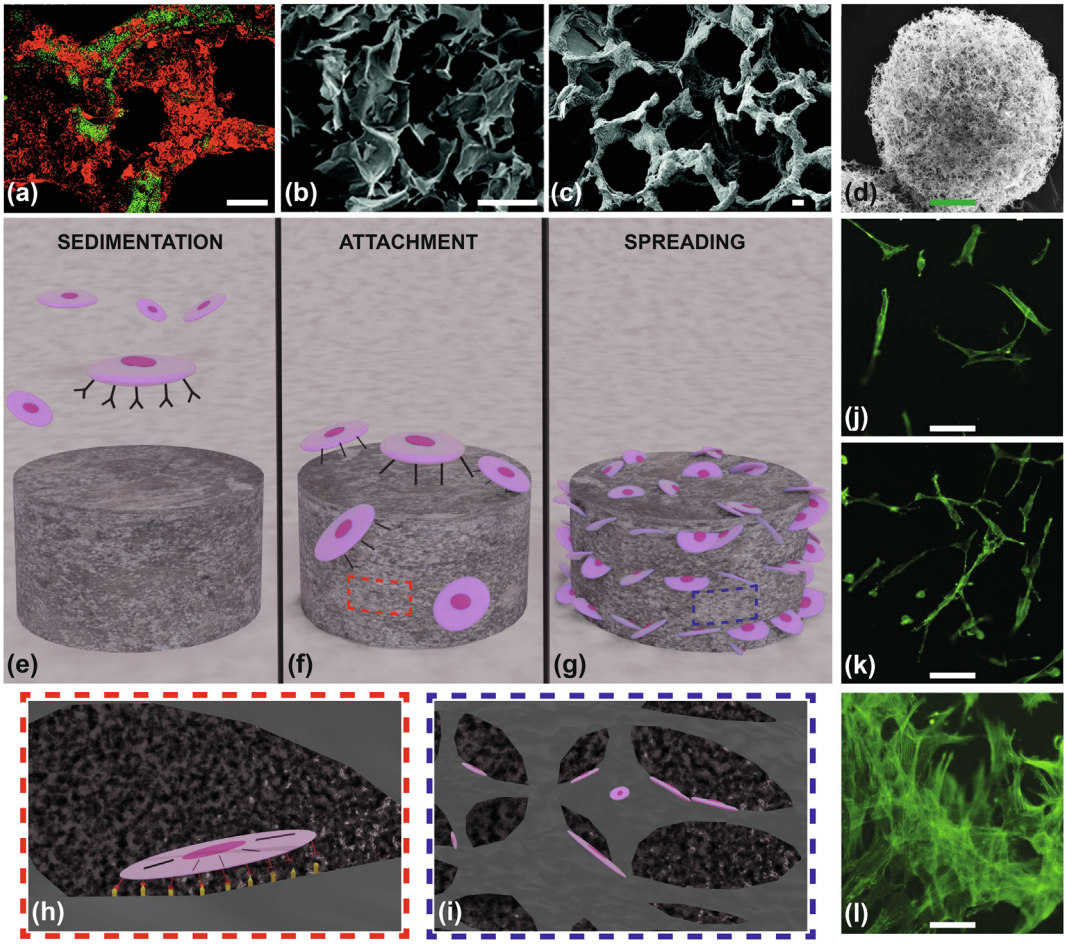

FIGURE 4

(a) Confocal, (b–d) scanning electron, and (j–l) epifluorescence microscopy images of nanocellulose-based scaffolds used in biomedical applications. (a) Osteoblast-like MG-63 cells (red) on the surfaces of CNC-coated scaffolds (green) after 2 weeks of cultivation; (b) cross-linked CNF scaffold; (c) bioactive glass scaffold coated with CNC; (d) CNF microspheres. (e–i) Main stages of *in vitro* cell adhesion, namely: (e) cell sedimentation; (f) attachment to the outer scaffold surface; (g) spreading over the outer scaffold surface; (h-i) inner scaffold surfaces indicated by the red and blue boxes. (j–l) Osteoblastic cells cultured on scaffolds for (j) 1, (k) 3, or (l) 7 days, with green fluorescence (Alexa Fluor 488-conjugated phalloidin) showing the actin cytoskeleton. White and green scale bars: 100 and 20 μm, respectively. (a and c) Adapted from Ref. [226] and (b) from Ref. [71], both published by the Royal Society of Chemistry; (d) Adapted from Ref. [94] with permission from the American Chemical Society; (j–l) Adapted from Ref. [230] with permission from Elsevier.

erate (Fig. 4j–l) [230]. Several variables play a role in scaffold biomedical performance, including the dispersant medium during scaffold preparation [231].

Specifically for bone tissue engineering, nanocellulose-based materials have been added into simulated body fluid (SBF) [232] as a route for the preparation of polymer/hydroxyapatite composites. Morimune-Moriya [233] prepared TEMPO-oxidized CNF with different contents of carboxyl groups and observed hydroxyapatite nucleation on the nanofibrils after immersion in SBF. Biologically, formation of layers of hydroxyapatite promote strong bonding with the surrounding bone tissue [234,235], given that hydroxyapatite is the mineralized component of bone [236,237]. Furthermore, hydroxyapatite layers can act in the expression of osteogenic genes [238,239] and stimulate angiogenesis [240–242]. Thus, hydroxyapatite nucleation can improve the scaffold performance [243]. Osorio et al. [217] prepared cross-linked CNC-only cryogel scaffolds capable of forming hydroxyapatite in SBF and increasing the osteosarcoma metabolism (Saos-2 cells), maintaining cell phenotype and improving *in vivo* bone growth by over 50% after 12 weeks implantation into non-load bearing cavities (Fig. 5a and b). Interestingly, comparing CNC bearing sulfate *versus* phosphate half ester surface groups did not alter cellulose's ability to nucleate hydroxyapatite *in vitro*, contrary to what might be expected from other reported phosphated bone scaffolds [217].

Bioactive glass has also been used to enhance the bonding of a biomaterial with the surrounding bone tissue [157,244,245]. This bioactive ceramic is a synthetic biomaterial used to mimic the porous structure of bones and to bond strongly to these, *in vivo* [246,247]. The ionic dissolution products of bioactive glass have been shown to have stimulatory properties on osteoblast proliferation and to act on osteogenic differentiation [248–250]. However, bioactive glass is typically stiff, brittle, and difficult to process into complex shapes. Hybrid materials combining the structure and properties of nanocellulose with the osteoconductive properties of bioactive glass indicate promising results in bone tissue engineering. Ferreira et al. [158] prepared highly interconnected CNF-based scaffolds containing bioactive glass

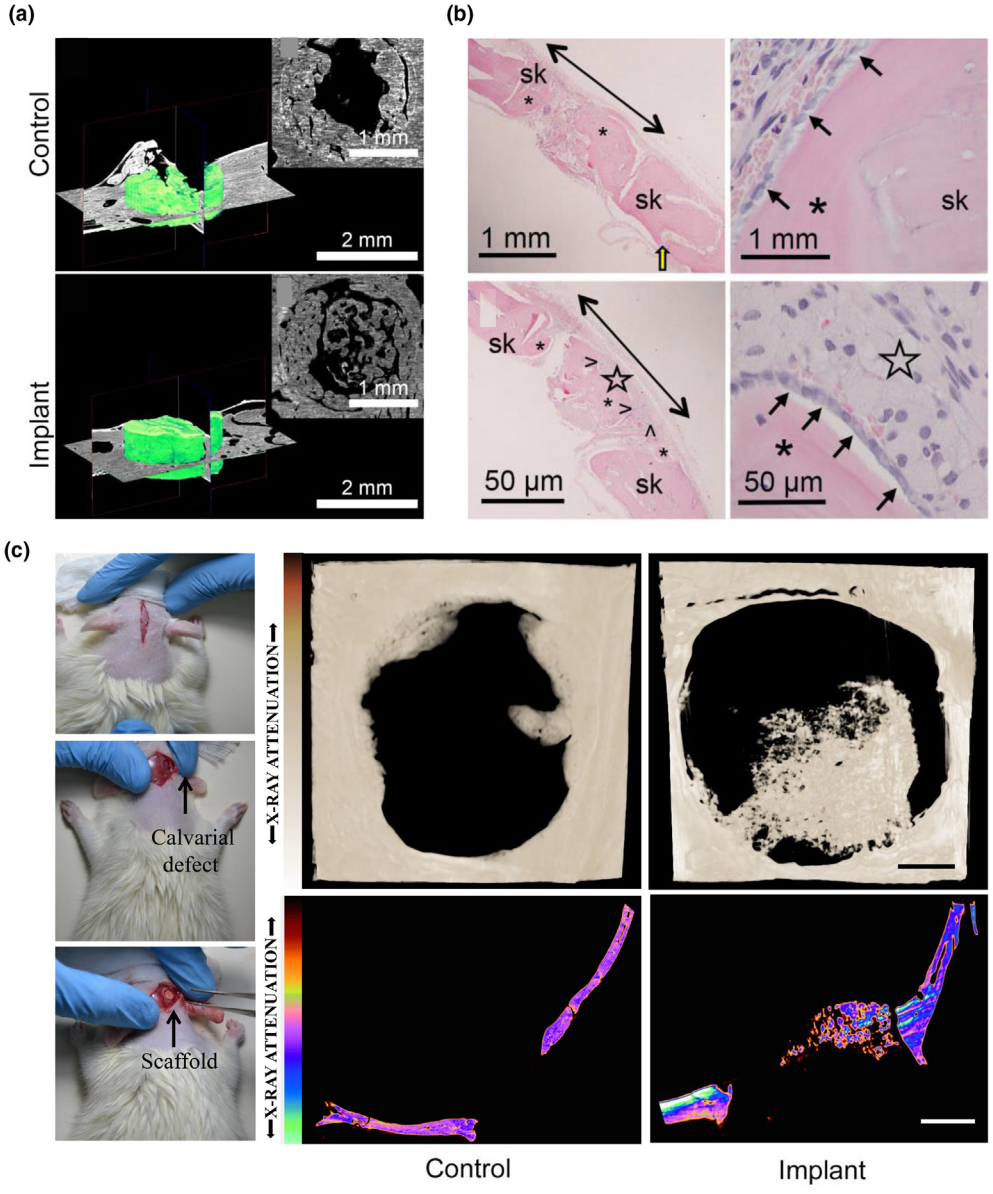

FIGURE 5

Representative X-ray micro-computed tomography reconstructions of *in vivo* calvarial defect models at (a) 56 and (c) 84 days showing bone mineralization in the groups treated with nanocellulose-based scaffolds (*i.e.*, Implant group). In (c), the X-ray attenuation data is red using as a reference a color gradient going from lower (top, black) to higher (bottom, green) attenuation values. Scale bars correspond to 1 mm. (b) histological slices confirming new bone growth and no signs of severe inflammation. (a and b) Adapted from Ref. [217] with permission from Elsevier; (c) adapted from Ref. [158] with permission from the Royal Society of Chemistry.

by freeze–casting. The authors confirmed that the hybrid material is cytocompatible with mouse osteoblastic cells (MC3T3-E1) and suitable for *in vivo* bone mineralization (Fig. 5**c**) owing to their morphology, good mechanical performance, and ability to form hydroxyapatite layers and to release Si, Ca, P, and Na ions from bioactive glass, which acted in osteogenic differentiation.

Nanocellulose-based scaffolds have also been researched for ligament, muscle, and cartilage tissue engineering. These tissues all have extremely different properties, and as such the ability to tune nanocellulose scaffold properties is of great importance. Naturally functioning human ligaments have a maximum elastic modulus in the 100s of MPa range, and a strain of 20–30%; this depends on factors such as age, gender, and physical activity [251]. Mathew et al. prepared partially regenerated CNF composites *via* sequential dissolution in ionic liquids and hot pressing [252]. These composites displayed similar mechanics (modulus between 300 and 500 MPa, strain between 20% and 25%) as native ligament, and were able to support the adhesion and proliferation of human ligament cells (HLC) and human vascular endothelial cells (HEC) – albeit not as well as tissue culture polystyrene controls. This research group also demonstrated similar results using hot-pressed CNF–collagen composite scaffolds [214].

Due to the relatively avascular nature of articular cartilage, this tissue has been a common target in developing materials

for tissue engineering, due to the prominent challenges associated with revascularizing a tissue [253]. Articular cartilage is composed mostly of extracellular matrix, with a few chondrocyte cells distributed throughout the tissue; and as a result also has a very limited capacity to repair itself. Here, scaffolds with pore sizes in the range of 200–300 μm and the ability to handle mechanical stresses up to 10 MPa are required. Naseri et al. [254] demonstrated the use of freeze–dried CNF–gelatin–chitosan scaffolds for the purpose of cartilage tissue engineering; these scaffolds had pore sizes between 75 and 200 μm and compressive moduli in the tens of kPa range in simulated body conditions. The scaffolds were also able to retain viable chondrocytes for up to 7 days. The same authors also demonstrated similar properties for CNF–alginate–gelatin composite scaffolds [255]. Ghafari et al. [256] prepared freeze–dried bilayer CNF–polyvinyl alcohol (PVA) aerogel scaffolds for skin tissue engineering. By varying the concentration of both CNF and PVA in the aerogels, the authors were able to control both the porosity (95% and 89%) and average pore size (90 and 20 μm) of the bilayers, aiming to mimic the dermis and epidermis, respectively [256].

Finally, of particular note, Camarero-Espinosa et al. [192] used thermally induced phase separation (TIPS) to prepare modular multi-layer scaffolds from polylactic acid (PLA) and CNC. By varying both the CNC surface chemistry (sulfated or phosphated) and TIPS methodology (solid–liquid or liquid–liquid) scaffolds could be prepared to mimic both the native chemistry and morphology of the different zones found in articular cartilage. Taken together, the chemical and structural cues provided in these multi-layer scaffolds were able to successfully direct the morphology, orientation, and phenotypic state of encapsulated chondrocytes; furthermore, after two weeks of culture, these scaffolds displayed mechanical properties similar to that of native healthy hyaline cartilage [192].

Commercial prospects of nanocellulose scaffolds as biomaterials

Fontana et al. [258] pioneered the use of BNC to temporarily replace damaged skin and paved the route for commercially available nanocellulose-based products (mostly from microbial synthesis) for biomedical applications, typically marketed for human skin repair, namely: Bionext® (Bennett Health, USA), Celmat® (BOWIL Biotech, Poland), Bioprocess® and DermaFill™ (Cellulose Solutions, USA), epicite^{hydro} (JeNaCell GmbH, Germany), Cuticell® Epigraft (BSN medical GmbH, Germany), Membracel® (Vuelo Pharma, Brazil), Nanocell® (Thai Nano Cellulose, Thailand), Nanoderm™ (Axcelon Biopolymers Corporation, Canada), and NEXFILL (Seven Biotecnologia, Brazil). This range of commercial products is suitable for different kinds of wounds, such as pressure sores, skin tears, venous stasis, diabetic wounds, skin graft donor sites, and traumatic abrasions [51,259]. The BNC-based dura mater implant SYNTHECEL® Dura Repair (DePuy Synthes, USA) and the BNC veterinary wound dressing for horses and dogs Cellumed® (Cellumed Co., South Korea) are also available commercially. Gengiflex® (Biofill, Brazil) two-layer membrane produced from pristine and alkali-modified BNC is a dental biomaterial intended to treat periodontal diseases through guided tissue regeneration (GTR), which reduces inflammatory responses in association with osseointegrated implants [260].

Although plant-derived nanocellulose scaffolds have the potential to meet the needs of tissue engineering, there has yet to be a breakthrough in the commercial market. To date, one of the only commercialized products is Growdex® (UPM Biomedicals, Finland) – a CNF-based product that is designed to support cell growth and differentiation. Encouragingly, there is a growing number of scientific articles (albeit still a small proportion) demonstrating promising *in vivo* performance of nanocellulose scaffolds for specific tissue engineering applications. However, further steps are required for a complete understanding about nanocelluloses as related to tissue growth synchrony, which is a complex phenomenon related to numerous micro-environmental cues [201,261]. Moreover, another remaining challenge is the establishment of clinical trials in humans.

The *in vivo* application of BNC in animal studies was first described by Roberts et al. [262], Yamanaka et al. [263], and Klemm et al. [264,265]. Subsequently, significant progress has been reported in experiments with rabbits [266], dogs [267], pigs [268], and other animals [259,269,270]. In these experiments, the polymer matrix was seeded with cells [267], and promising results were also achieved with cell-free implants [271]. Lee et al. [272] reported on the use of BNC membranes for GTR on rat calvarial defects, maintaining a suitable opening for bone regeneration while not provoking inflammatory responses. Similarly, Zhang et al. [273] used BNC membranes to induce GTR and repair maxillary canine periodontal defects in beagle dog breeds. BNC also exhibited good acceptance and adherence to bone graft fragments when used as a substitute for dura mater in mongrel dogs [274]. Successful *in vivo* tissue engineering applications in human regenerative medicine were also observed in a multicenter clinical trial in the USA [275]. Rosen et al. [275] reported on a 6-month study wherein BNC devices were compared with commercially available dural replacements. While the BNC devices did not present inferior results compared with their commercial counterparts, longer-term data are needed to identify potential limitations of the use of BNC in humans [275]. This promising progress and successful deployment of BNC biomaterials strongly supports the possible adoption of CNF- and CNC-based scaffolds in future biomedical products.

The translation from laboratory technology to the clinic is a time consuming and costly step due to the necessity for regulatory authorization/approval following production trials requiring special infrastructure, which is often out of reach for academic researchers [150]. However, any such translation should eventually result in financial stimulus, as the sales of biomaterials for tissue engineering already exceeds US$ 240 million per year [276]. Furthermore, by 2040, 25% of the US GDP is expected to be related to healthcare [276,277]. Therefore, the gap between research and commercialization may be interesting to overcome.

Remarks and perspectives

Significant progress has been made towards the establishment of nanocellulose-based scaffolds for tissue regeneration. Scaffold-forming methods that allow for the fine-tuning of structural

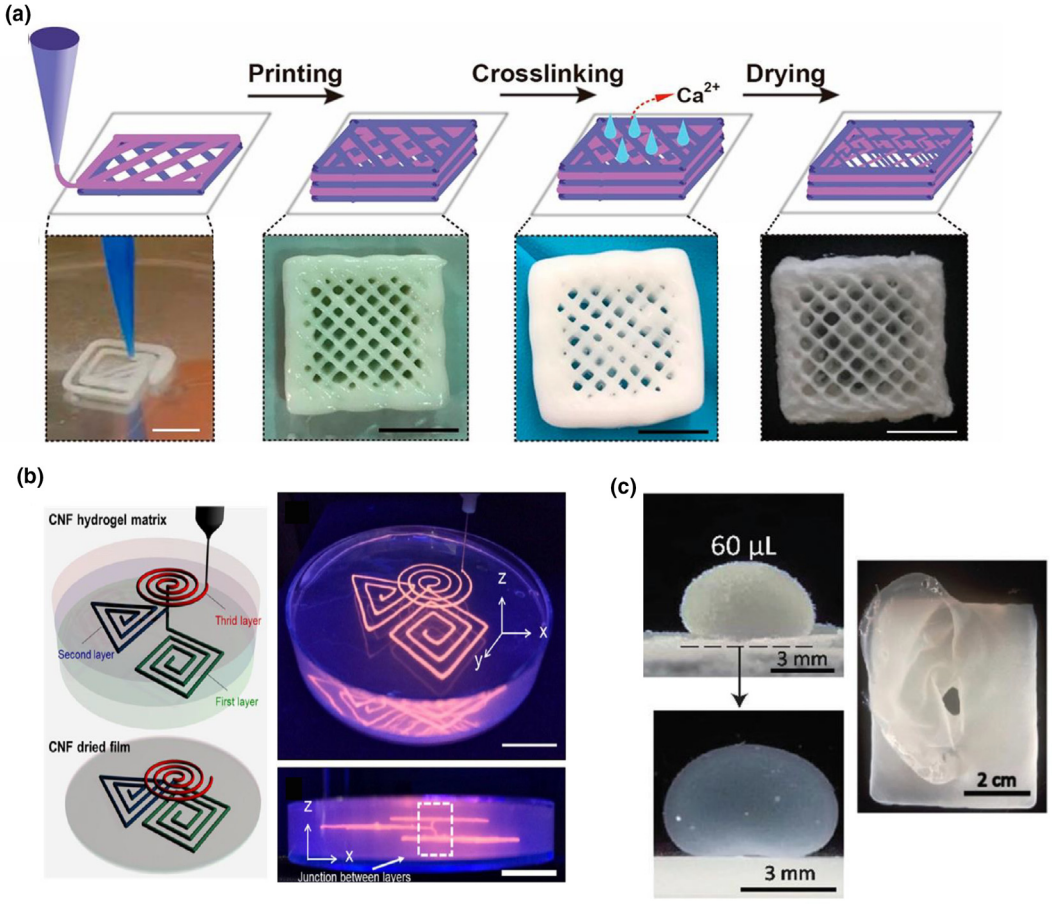

FIGURE 6

(a) 3D printing of CNF-based emulsion gels into cubic scaffolds. (b) CNF hydrogels used to support printed structures. (c) Biofabrication of capsules and customizable 3D nanocellulose structures. Adapted from (a) Ref. [287] (b) Ref. [278] with permission from the American Chemical Society. (c) Adapted from Ref. [291] with permission from the Royal Society of Chemistry.

and mechanical features have been demonstrated, opening numerous possibilities for future applications. However, challenges still remain for the preparation of materials combining high porosity and suitable mechanical performance. Additionally, further *in vitro* and *in vivo* studies are required and the gap between research and commercialization needs to be bridged.

Additive manufacturing and biofabrication have emerged as promising routes for the preparation of nanocellulose-based materials for tissue engineering (Fig. 6) [278–281]. 3D printing is highly attractive for biomedical purposes because the shape and morphology of the materials can be customized at different levels [282–285]. Efforts have been made towards realizing 3D printed materials for bone regeneration, such as collagen-based scaffolds loaded with bone marrow stem cells that serve as *ex situ* miRNA delivery systems and improved bone regeneration in rats [286]. However, the control over the dimensional stability of the resulting materials after printing, due to shrinkage/swelling, is a challenge that still needs to be overcome. Nanocellulose can be used to control the rheological properties of an ink, allowing high printing fidelity and shape stability [137,287–289]. Several research groups have demonstrated 3D printed CNF/alginate composite hydrogels with human chondrocytes to form anatomically shaped cartilage scaffolds [138,290]. These scaffolds had storage moduli between 10 and 60 kPa and were able to retain viable chondrocyte cells for up to 28 days post 3D printing.

Biofabrication using BNC-producing bacteria is another powerful route to prepare customizable nanocellulosic structures with the advantage of the improved control over the 3D morphology and the possibility of achieving complex geometries when compared to 3D printing [291]. By using such methodology, biofilm fabrication is stabilized at the air–water interface through hydrophobic particles, allowing the preparation of complex and engineerable morphologies that may be suitable for biomedical applications [292,293]. Additionally, combining emulsion inks and 3D printing [294,295], direct 3D printing of aerogels [280,296], or lithographic patterning of aerogels [297] represent feasible approaches to create scaffolds with dual or hierarchical morphologies that would not be attainable using one single technique.

Another trend in this context encompasses materials that have their rheological properties controlled in a way that they can be injected into the human body without the need for surgery, as exemplified by De France et al. [173,218,219], who prepared injectable hydrogels from synthetic poly(oligoethylene glycol methacrylate) and CNC. By utilizing the diamagnetic anisotropy of CNC, the authors were able to align the nanocrystals

in situ within the hydrogel network. This magnetic alignment resulted in anisotropic mechanical properties, as seen in native muscle, and supported the directional growth and differentiation of C2C12 mouse myoblast cells [218].

Exploring new combinations of nanocellulose, ceramics or polymers to design composite scaffolds with controlled porosity and tailored properties for specific applications is also expected to contribute to further developments in this field. As for bioactivity, the addition of bioactive materials such as hydroxyapatite and bioactive glass can remarkably improve the osteoconductivity of nanocellulose scaffolds, standing out as a promising strategy to promote the use of such materials for tissue regeneration. Moreover, to achieve improved biodegradation, the addition of ceramic materials and degradable polymers should improve the overall scaffold degradation rate. Alternatively, new materials with nanocellulose acting as a biotemplate can also be developed. New frontiers of research in drug delivery systems can also be directed using the improved biodegradation of nanocellulose scaffolds in a time-dependent manner.

As discussed in this review, dried nanocellulose-based gels and foams are biocompatible, non-cytotoxic, and overall promising as scaffolds in biomedical applications. However, some attention needs to be given to the biodegradability *in vivo*. This is especially considering that a foreign material in the body may lead to inflammatory responses, damaging therefore the tissue regeneration. Several polymer matrices have been used as scaffolds, including poly(D,L-lactic-*co*-glycolic acid) and poly(ε-caprolactone), which degrade in the body and lead to cell viability and low inflammatory effects that are related to this degradation rate [298]. Because nanocellulose is biodurable [111], more studies on the inflammatory effect of its scaffolds are needed for their commercial success as biomaterials. An interesting means of overcoming this hurdle is the simple supplementation of nanocellulose scaffolds with cyto-compatible cellulose-degrading enzymes targeting *in vivo* degradation [17].

Finally, compared to soluble polymers that undergo *in vivo* degradation, it is remarkable that nanocellulose maintains its inherent multi-level hierarchical assembly, potentially providing exclusive features such as structural integrity and wet resilience. Nevertheless, this architecture is not unique to cellulose and can also be found in other progressively deconstructed nanostructured polysaccharides, including chitin, with the advantage that chitin is known to degrade at physiological conditions [299]. Notable efforts have been made lately in the use of nanochitin to produce porous materials [90,300], much of those catalyzed by the previous knowledge on the behavior of nanocellulose for the same purpose given the high similarity among both polysaccharides. Altogether, these aspects point towards nanochitin and nanocellulose as promising building blocks for scaffolds intended for tissue engineering.

Declaration of Competing Interest

The authors declare that they have no known competing financial interests or personal relationships that could have appeared to influence the work reported in this paper.

Acknowledgements

The authors acknowledge the financial support from the São Paulo Research Foundation [FAPESP; Grants No. 2016/09588-9, 2018/16851-3, 2018/12831-8, 2018/25512-8, and 2019/00370-1], the Brazilian National Council for Scientific and Technological Development (CNPq), the Natural Sciences and Engineering Research Council of Canada, and the European Research Council [ERC; under the European Union's Horizon 2020 Research and Innovation Programme, ERC Advanced Grant agreement No. 788489, "BioElCell"].

References

[1] J.Q. Yin, J. Zhu, J.A. Ankrum, Nat. Biomed. Eng. 3 (2019) 90–104.
[2] J. Koffler et al., Nat. Med. 25 (2019) 263–269.
[3] M. Long, H. Rack, Biomaterials 19 (1998) 1621–1639.
[4] J. Hanker, B. Giammara, Science (80-.). 242 (1988) 885–892.
[5] M. Montgomery et al., Nat. Mater. 16 (2017) 1038–1046.
[6] H. Jinnouchi et al., Nat. Rev. Cardiol. 16 (2019) 286–304.
[7] D.B. Kolesky et al., Adv. Mater. 26 (2014) 3124–3130.
[8] Y. Shin et al., Adv. Healthc. Mater. 2 (2013) 790–794.
[9] P. Podsiadlo, et al., Science (80-.). 318 (2007) 80–83.
[10] H. Sai, et al., Science (80-.). 341 (2013) 530–534.
[11] N. Mitrousis, A. Fokina, M.S. Shoichet, Nat. Rev. Mater. 3 (2018) 441–456.
[12] F.M. Wunner et al., Adv. Mater. 30 (2018) 1706570.
[13] N. Ashammakhi et al., Adv. Healthc. Mater. 8 (2019) 1801048.
[14] L.C.M. Lebreton et al., Nat. Commun. 8 (2017) 15611.
[15] R. Geyer, J.R. Jambeck, K.L. Law, Sci. Adv. 3 (2017) e1700782.
[16] T. Keplinger, X. Wang, I. Burgert, J. Mater. Chem. A 7 (2019) 2981–2992.
[17] E. Entcheva et al., Biomaterials 25 (2004) 5753–5762.
[18] N. Lavoine, L. Bergström, J. Mater. Chem. A 5 (2017) 16105–16117.
[19] N. Buchtová, T. Budtova, Cellulose 23 (2016) 2585–2595.
[20] N. Lin, A. Dufresne, Eur. Polym. J. 59 (2014) 302–325.
[21] A. Tripathi et al., J. Mater. Chem. A 7 (2019) 15309–15319.
[22] N.T. Cervin et al., Biomacromolecules 14 (2013) 503–511.
[23] M. Pääkkö et al., Soft Matter 4 (2008) 2492.
[24] T. Lu et al., Compos. Sci. Technol. 94 (2014) 132–138.
[25] A.J. Svagan, M.A.S.A. Samir, L.A. Berglund, Adv. Mater. 20 (2008) 1263–1269.
[26] K.J. De France, T. Hoare, E.D. Cranston, Chem. Mater. 29 (2017) 4609–4631.
[27] T. Budtova, Cellulose 26 (2019) 81–121.
[28] S. Gupta et al., Appl. Sci. 8 (2018) 2463.
[29] L.-Y. Long, Y.-X. Weng, Y.-Z. Wang, Polymers (Basel). 10 (2018) 623.
[30] R.M.A. Domingues, M.E. Gomes, R.L. Reis, Biomacromolecules 15 (2014) 2327–2346.
[31] A. Brongniart, T.-J. Pelouze, J.-B.A. Dumas, C. R. Acad. Sci. 8 (1839) 51–53.
[32] D. Roy et al., Chem. Soc. Rev. 38 (2009) 2046.
[33] E. Kontturi et al., Adv. Mater. 30 (2018) 1703779.
[34] Y. Habibi, L.A. Lucia, O.J. Rojas, Chem. Rev. 110 (2010) 3479–3500.
[35] M. Jorfi, E.J. Foster, J. Appl. Polym. Sci. 132 (2015) 1–19.
[36] B. Thomas et al., Chem. Rev. 118 (2018) 11575–11625.
[37] S.J. Eichhorn et al., J. Mater. Sci. 45 (2010) 1–33.
[38] A.J. Onyianta, M. Dorris, R.L. Williams, Cellulose 25 (2018) 1047–1064.
[39] X. Liu et al., Carbohydr. Polym. 208 (2019) 191–199.
[40] O. Nechyporchuk, M.N. Belgacem, J. Bras, Ind. Crops Prod. 93 (2016) 2–25.
[41] H.P.S. Abdul Khalil et al., Carbohydr. Polym. 99 (2014) 649–665.
[42] J. Desmaisons et al., Carbohydr. Polym. 174 (2017) 318–329.
[43] M. Jonoobi et al., Cellulose 22 (2015) 935–969.
[44] I. Usov et al., Nat. Commun. 6 (2015) 7564.
[45] O. Nechyporchuk, M.N. Belgacem, F. Pignon, Biomacromolecules 17 (2016) 2311–2320.
[46] F.V. Ferreira et al., Appl. Surf. Sci. 436 (2018) 1113–1122.
[47] A. Šturcová, G.R. Davies, S.J. Eichhorn, Biomacromolecules 6 (2005) 1055–1061.
[48] E.J. Foster et al., Chem. Soc. Rev. 47 (2018) 2609–2679.
[49] M.S. Reid, M. Villalobos, E.D. Cranston, Langmuir 33 (2017) 1583–1598.
[50] M. Pääkkö et al., Biomacromolecules 8 (2007) 1934–1941.
[51] H.G. de Oliveira Barud et al., Carbohydr. Polym. 153 (2016) 406–420.
[52] D. Klemm et al., Mater. Today 21 (2018) 720–748.
[53] J. Araki, S. Kuga, Langmuir 17 (2001) 4493–4496.
[54] C.A. de Assis et al., Biofuels Bioprod. Biorefin. 12 (2018) 251–264.

[55] C.A. de Assis et al., Biofuels, Bioprod. Biorefin. 11 (2017) 682–700.
[56] F. Hoeng, A. Denneulin, J. Bras, Nanoscale 8 (2016) 13131–13154.
[57] H. Kargarzadeh et al., Prog. Polym. Sci. 87 (2018) 197–227.
[58] S. Boufi et al., Carbohydr. Polym. 154 (2016) 151–166.
[59] A.W. Carpenter, C.-F. de Lannoy, M.R. Wiesner, Environ. Sci. Technol. 49 (2015) 5277–5287.
[60] H. Voisin et al., Nanomaterials 7 (2017) 57.
[61] W. Chen et al., Chem. Soc. Rev. 47 (2018) 2837–2872.
[62] N. Lavoine et al., Carbohydr. Polym. 149 (2016) 40–50.
[63] N.T. Cervin et al., Cellulose 19 (2012) 401–410.
[64] H. Sehaqui et al., Soft Matter 6 (2010) 1824.
[65] X. Yang, E.D. Cranston, Chem. Mater. 26 (2014) 6016–6025.
[66] H. Valo et al., Eur. J. Pharm. Sci. 50 (2013) 69–77.
[67] C.A. García-González, M. Alnaief, I. Smirnova, Carbohydr. Polym. 86 (2011) 1425–1438.
[68] B. Wicklein et al., Nat. Nanotechnol. 10 (2015) 277–283.
[69] N. Mahfoudhi, S. Boufi, Cellulose 24 (2017) 1171–1197.
[70] H. Maleki, Chem. Eng. J. 300 (2016) 98–118.
[71] J.C. Courtenay et al., J. Mater. Chem. B 7 (2019) 53–64.
[72] E. Avcu et al., Prog. Mater. Sci. 103 (2019) 69–108.
[73] S. Bose et al., Prog. Mater. Sci. 93 (2018) 45–111.
[74] J. Ni et al., Mater. Today Biol. 3 (2019) 100024.
[75] O. Faruk, A.K. Bledzki, L.M. Matuana, Macromol. Mater. Eng. 292 (2007) 113–127.
[76] S. Groult, Pectin-Based Aerogels: Advanced Materials for Thermal Insulation and Drug Delivery Applications, MINES ParisTech (2019).
[77] I. Kalashnikova et al., Langmuir 27 (2011) 7471–7479.
[78] A.M. Al-Qararah et al., Colloids Surf., A Physicochem. Eng. Asp. 436 (2013) 1130–1139.
[79] A.M. Al-Qararah et al., Colloids Surf., A Physicochem. Eng. Asp. 482 (2015) 544–553.
[80] F. Martoïa et al., Mater. Des. 104 (2016) 376–391.
[81] M. Mariano et al., Carbohydr. Polym. 195 (2018) 153–162.
[82] K.S. Gordeyeva et al., J. Colloid Interface Sci. 472 (2016) 44–51.
[83] J. Li et al., Ind. Crops Prod. 128 (2019) 186–193.
[84] K. Kriechbaum et al., ACS Sustainable Chem. Eng. 6 (2018) 11959–11961.
[85] Y. Kobayashi, T. Saito, A. Isogai, Angew. Chem., Int. Ed. 53 (2014) 10394–10397.
[86] N. Buchtová et al., Soft Matter 15 (2019) 7901–7908.
[87] C. Darpentigny et al., Carbohydr. Polym. (2019) 115560.
[88] D.A. Osorio et al., J. Mater. Sci. 53 (2018) 9842–9860.
[89] S. Deville, J. Mater. Res. 28 (2013) 2202–2219.
[90] L. Liu et al., ACS Nano 13 (2019) 2927–2935.
[91] L. Lewis et al., ACS Macro Lett. (2019) 486–491.
[92] X. Wu et al., Acta Biomater. 6 (2010) 1167–1177.
[93] M.C. Gutiérrez et al., Langmuir 25 (2009) 5509–5515.
[94] H. Cai et al., Biomacromolecules 15 (2014) 2540–2547.
[95] C. Jiménez-Saelices et al., Carbohydr. Polym. 157 (2017) 105–113.
[96] D. Levin et al., Chem. Mater. 30 (2018) 8040–8051.
[97] J. Lindh et al., Langmuir 32 (2016) 5600–5607.
[98] J. Erlandsson et al., Appl. Mater. Today 5 (2016) 246–254.
[99] S. Deville, Materials (Basel) 3 (2010) 1913–1927.
[100] P. Munier et al., Biomacromolecules 17 (2016) 1875–1881.
[101] M. Chau et al., Chem. Mater. 28 (2016) 3406–3415.
[102] S. Deville et al., Science (80-) 311 (2006) 515–518.
[103] N.T. Cervin et al., Biomacromolecules 16 (2015) 822–831.
[104] H.-D. Jung et al., Mater. Lett. 63 (2009) 1545–1547.
[105] E. Munch et al., J. Am. Ceram. Soc. 92 (2009) 1534–1539.
[106] K.M. Pawelec et al., J. Mater. Sci. 50 (2015) 7537–7543.
[107] B. Chen et al., RSC Adv. 6 (2016) 96518–96526.
[108] M. Mariano, J. da S. Bernardes, M. Strauss, Mater. Lett. 225 (2018) 167–170.
[109] C.G. Otoni et al., ACS Appl. Bio Mater. 2 (2019) 1975–1986.
[110] Y.S. Song et al., Proc. Natl. Acad. Sci. U.S.A. 107 (2010) 4596–4600.
[111] J.G. Torres-Rendon et al., Adv. Mater. 27 (2015) 2989–2995.
[112] E.J. Foster, N. Zahed, C. Tallon, Small 14 (2018) 1802068.
[113] M. Giese et al., Angew. Chem., Int. Ed. 54 (2015) 2888–2910.
[114] J.G. Torres-Rendon et al., Biomacromolecules 17 (2016) 905–913.
[115] J. Wu et al., Cellulose 26 (2019) 2513–2528.
[116] S. Khan et al., Int. J. Biol. Macromol. 117 (2018) 1200–1210.
[117] S. Khan et al., RSC Adv. 6 (2016) 110840–110849.
[118] Z. Xu et al., RSC Adv. 6 (2016) 43626–43633.
[119] Y. Wang et al., Carbohydr. Polym. 167 (2017) 44–51.
[120] N. Pircher et al., Macromol. Mater. Eng. 300 (2015) 911–924.
[121] S. Zadegan et al., Mater. Sci. Eng. C 31 (2011) 954–961.
[122] M. Zaborowska et al., Acta Biomater. 6 (2010) 2540–2547.
[123] N. Annabi et al., Tissue Eng. Part B 16 (2010) 371–383.
[124] K.J. De France, F. Xu, T. Hoare, Adv. Healthc. Mater. 7 (2018) 1–17.
[125] H.P.S.A. Khalil, Y. Davoudpour, A.H. Bhat, E. Rosamah, P.M. Tahir, in: Handb. Polym. Nanocomposites. Process. Perform. Appl., Springer Berlin Heidelberg, Berlin, Heidelberg, 2015, pp. 191–227.
[126] A. Hivechi, S.H. Bahrami, R.A. Siegel, Int. J. Biol. Macromol. 124 (2019) 411–417.
[127] F. Ahmed et al., Carbohydr. Polym. 115 (2015) 388–393.
[128] X. He et al., Carbohydr. Polym. 115 (2015) 485–493.
[129] M. Ago et al., Biomacromolecules 13 (2012) 918–926.
[130] C. Li et al., Materials (Basel) 10 (2017) 572.
[131] X. He et al., Biomacromolecules 15 (2014) 618–627.
[132] S. Huan et al., Biomacromolecules 19 (2018) 1037–1046.
[133] S. Sultan et al., Curr. Opin. Biomed. Eng. 2 (2017) 29–34.
[134] S. Sultan, A.P. Mathew, Nanoscale 10 (2018) 4421–4431.
[135] W. Xu et al., ACS Appl. Mater. Interfaces 11 (2019) 8838–8848.
[136] M. Ojansivu et al., Biofabrication 11 (2019) 035010.
[137] G. Siqueira et al., Adv. Funct. Mater. 27 (2017) 1604619.
[138] K. Markstedt et al., Biomacromolecules 16 (2015) 1489–1496.
[139] A.I. Cernencu et al., Carbohydr. Polym. 220 (2019) 12–21.
[140] J. Wang et al., Angew. Chem., Int. Ed. 57 (2018) 2353–2356.
[141] G.-Q. Chen, Chem. Soc. Rev. 38 (2009) 2434.
[142] E.S. Place et al., Chem. Soc. Rev. 38 (2009) 1139.
[143] M.M. Stevens, Mater. Today 11 (2008) 18–25.
[144] K.J. Burg, S. Porter, J.F. Kellam, Biomaterials 21 (2000) 2347–2359.
[145] A. Khademhosseini, R. Langer, Biomaterials 28 (2007) 5087–5092.
[146] F. Brandl, F. Sommer, A. Goepferich, Biomaterials 28 (2007) 134–146.
[147] S.J. Hollister, Nat. Mater. 4 (2005) 518–524.
[148] Q.L. Loh, C. Choong, Tissue Eng. Part B Rev. 19 (2013) 485–502.
[149] V. Liu Tsang, S.N. Bhatia, Adv. Drug Deliv. Rev. 56 (2004) 1635–1647.
[150] L. Roseti et al., Mater. Sci. Eng. C 78 (2017) 1246–1262.
[151] M.B. Ginzberg, R. Kafri, M. Kirschner, Science (80-) 348 (2015). 1245075–1245075.
[152] A.J. Engler et al., Cell 126 (2006) 677–689.
[153] U.G.K. Wegst et al., Nat. Mater. 14 (2015) 23–36.
[154] K.J. Koester, J.W. Ager, R.O. Ritchie, Nat. Mater. 7 (2008) 672–677.
[155] L.J. Gibson, J. Biomech. 18 (1985) 317–328.
[156] E.B. Giesen et al., J. Biomech. 34 (2001) 799–803.
[157] K. Rezwan et al., Biomaterials 27 (2006) 3413–3431.
[158] F.V. Ferreira et al., Nanoscale 11 (2019) 19842–19849.
[159] J. Liu et al., Carbohydr. Polym. 148 (2016) 259–271.
[160] C. Huang et al., RSC Adv. 9 (2019) 5786–5793.
[161] Y. Zhou et al., RSC Adv. 3 (2013) 19272.
[162] C. Darpentigny et al., Cellulose (2019).
[163] Y. Huang et al., ACS Sustainable Chem. Eng. 6 (2018) 10552–10561.
[164] U.-J. Kim et al., Biomaterials 26 (2005) 2775–2785.
[165] T.G. van Tienen et al., Biomaterials 23 (2002) 1731–1738.
[166] I. Sabree, J.E. Gough, B. Derby, Ceram. Int. 41 (2015) 8425–8432.
[167] E. Gregorová et al., J. Eur. Ceram. Soc. 36 (2016) 109–120.
[168] V. Sciamanna, B. Nait-Ali, M. Gonon, Ceram. Int. 41 (2015) 2599–2606.
[169] X. Zhang et al., Mater. Sci. Eng. C 42 (2014) 362–367.
[170] J.C. Li, D.C. Dunand, Acta Mater. 59 (2011) 146–158.
[171] A. Rashad et al., Biomacromolecules 18 (2017) 1238–1248.
[172] S.F. Souza et al., Carbohydr. Polym. 201 (2018) 87–95.
[173] K.J. De France et al., ACS Biomater. Sci. Eng. 5 (2019) 2235–2246.
[174] S. Camarero-Espinosa et al., Fibers 4 (2016) 21.
[175] K.A. Mahmoud et al., ACS Appl. Mater. Interfaces 2 (2010) 2924–2932.
[176] M. Roman, Ind. Biotechnol. 11 (2015) 25–33.
[177] M. Roman et al., Nano Life 2 (2012) 1241006.
[178] K. Hannukainen et al., Environ. Mol. Mutagen. 56 (2015) 171–182.
[179] L. Colombo et al., Biomacromolecules 16 (2015) 2862–2871.
[180] J. Athinarayanan, V.S. Periasamy, A.A. Alshatwi, Int. J. Biol. Macromol. 117 (2018) 911–918.
[181] C. Ventura et al., Toxicol. Lett. 291 (2018) 173–183.
[182] H. Ni et al., Biomed. Mater. Eng. 22 (2012) 121–127.
[183] M.M. Pereira et al., Nanotechnology 24 (2013) 075103.
[184] M. Ogonowski et al., Nanotoxicology 12 (2018) 509–521.
[185] Z. Hanif et al., Colloids Surf. B: Biointerfaces 119 (2014) 162–165.
[186] J. Catalán et al., Mutagenesis 32 (2017) 23–31.
[187] R. Koshani, A. Madadlou, Trends Food Sci. Technol. 71 (2018) 268–273.

[188] B. O'Connor, R. Berry, R. Goguen, in: Nanotechnol. Environ. Heal. Saf. (Second Ed., 2014, pp. 225–246.
[189] C. Endes et al., Biomacromolecules 16 (2015) 1267–1275.
[190] N. Yanamala et al., ACS Sustainable Chem. Eng. 2 (2014) 1691–1698.
[191] G.M. DeLoid et al., Environ. Sci. Nano 6 (2019) 2105–2115.
[192] S. Camarero-Espinosa et al., Biomaterials 74 (2016) 42–52.
[193] I. Armentano et al., Polym. Degrad. Stab. 95 (2010) 2126–2146.
[194] V. Maquet et al., Biomaterials 25 (2004) 4185–4194.
[195] P.X. Ma, Mater. Today 7 (2004) 30–40.
[196] J.L. Drury, D.J. Mooney, Biomaterials 24 (2003) 4337–4351.
[197] E. Lam et al., Trends Biotechnol. 30 (2012) 283–290.
[198] L.R. Madden et al., Proc. Natl. Acad. Sci. U.S.A. 107 (2010) 15211–15216.
[199] C. Zhu et al., Adv. Mater. 30 (2018) 1707306.
[200] F. Causa, P.A. Netti, L. Ambrosio, Biomaterials 28 (2007) 5093–5099.
[201] N. Nasiri et al., ACS Appl. Mater. Interfaces 10 (2018) 24840–24849.
[202] C.M. Murphy, M.G. Haugh, F.J. O'Brien, Biomaterials 31 (2010) 461–466.
[203] B.B. Mandal, S.C. Kundu, Biomaterials 30 (2009) 2956–2965.
[204] O. Oliviero, M. Ventre, P.A. Netti, Acta Biomater. 8 (2012) 3294–3301.
[205] A. Artel et al., Tissue Eng. Part A 17 (2011) 2133–2141.
[206] X.-Y. Yang et al., Chem. Soc. Rev. 46 (2017) 481–558.
[207] V. Karageorgiou, D. Kaplan, Biomaterials 26 (2005) 5474–5491.
[208] J. Tang et al., Carbohydr. Polym. 208 (2019) 404–412.
[209] Z. Hu et al., ACS Macro Lett. 5 (2016) 185–189.
[210] M. Hamedi et al., Angew. Chem., Int. Ed. 52 (2013) 12038–12042.
[211] Y. Kim et al., Chem. Eng. J. 313 (2017) 1042–1050.
[212] N.T. Cervin et al., ACS Appl. Mater. Interfaces 8 (2016) 11682–11689.
[213] W. Zhang et al., J. Mater. Chem. 22 (2012) 11642.
[214] A.P. Mathew et al., Macromol. Biosci. 13 (2013) 289–298.
[215] M. Park et al., Colloids Surfaces B Biointerfaces 130 (2015) 222–228.
[216] X. Yang et al., Adv. Mater. 27 (2015) 6104–6109.
[217] D.A. Osorio et al., Acta Biomater. 87 (2019) 152–165.
[218] K.J. De France et al., Nano Lett. 17 (2017) 6487–6495.
[219] K.J. De France et al., Biomacromolecules 17 (2016) 649–660.
[220] A. Fabbro et al., ACS Nano 6 (2012) 2041–2055.
[221] M.A. Pattison et al., Biomaterials 26 (2005) 2491–2500.
[222] B.D. Boyan, E.M. Lotz, Z. Schwartz, Tissue Eng. Part A 23 (2017) 1479–1489.
[223] Z. Schwartz et al., Adv. Dent. Res. 13 (1999) 38–48.
[224] J.M. Dugan et al., Acta Biomater. 9 (2013) 4707–4715.
[225] J.M. Dugan, J.E. Gough, S.J. Eichhorn, Biomacromolecules 11 (2010) 2498–2504.
[226] W. Li et al., RSC Adv. 4 (2014) 56156–56164.
[227] W. Li et al., J. Eur. Ceram. Soc. 34 (2014) 505–514.
[228] Q.Z. Chen, I.D. Thompson, A.R. Boccaccini, Biomaterials 27 (2006) 2414–2425.
[229] A. Khalili, M. Ahmad, Int. J. Mol. Sci. 16 (2015) 18149–18184.
[230] S. Saska et al., Int. J. Biol. Macromol. 103 (2017) 467–476.
[231] H.J. Kim et al., Biomaterials 26 (2005) 4442–4452.
[232] T. Kokubo, H. Takadama, Biomaterials 27 (2006) 2907–2915.
[233] S. Morimune-Moriya et al., Polym. J. 47 (2015) 158–163.
[234] L.L. Hench, H.A. Paschall, J. Biomed. Mater. Res. 7 (1973) 25–42.
[235] F.E. Ciraldo et al., Acta Biomater. 75 (2018) 3–10.
[236] H.H. Lu et al., J. Biomed. Mater. Res. 64A (2003) 465–474.
[237] A. Boccaccini, Compos. Sci. Technol. 63 (2003) 2417–2429.
[238] I.D. Xynos et al., J. Biomed. Mater. Res. 55 (2001) 151–157.
[239] G. Jell, M.M. Stevens, J. Mater. Sci. Mater. Med. 17 (2006) 997–1002.
[240] L.L. Hench, Biomed. Glas. 1 (2015).
[241] J. Kentleach et al., Biomaterials 27 (2006) 3249–3255.
[242] Q. Fu et al., Mater. Sci. Eng. C 31 (2011) 1245–1256.
[243] J.M. Holzwarth, P.X. Ma, Biomaterials 32 (2011) 9622–9629.
[244] J.J. Chung et al., Chem. Mater. 28 (2016) 6127–6135.
[245] F. Hajiali, S. Tajbakhsh, A. Shojaei, Polym. Rev. (2017) 1–44.
[246] L. Hench, J. Wilson, Science (80-) 226 (1984) 630–636.
[247] J.N. Harvestine et al., Biomacromolecules 17 (2016) 3524–3531.
[248] O. Tsigkou et al., Biomaterials 30 (2009) 3542–3550.
[249] Á.J. Leite et al., ACS Appl. Mater. Interfaces 10 (2018) 23311–23320.
[250] A.A. Gorustovich, J.A. Roether, A.R. Boccaccini, Tissue Eng. Part B Rev. 16 (2010) 199–207.
[251] D.L. Butler, M.D. Kay, D.C. Stouffer, J. Biomech. 19 (1986) 425–432.
[252] A.P. Mathew et al., Carbohydr. Polym. 87 (2012) 2291–2298.
[253] D.J. Huey, J.C. Hu, K.A. Athanasiou, Science (80-) 338 (2012) 917–921.
[254] N. Naseri et al., RSC Adv. 6 (2016) 5999–6007.
[255] N. Naseri et al., Biomacromolecules 17 (2016) 3714–3723.
[256] R. Ghafari et al., Int. J. Biol. Macromol. 136 (2019) 796–803.
[257] Y. Shan et al., RSC Adv. 9 (2019) 22966–22979.
[258] J.D. Fontana et al., Appl. Biochem. Biotechnol. 24–25 (1990) 253–264.
[259] W. Czaja et al., Biomaterials 27 (2006) 145–151.
[260] A.B. Novaes Jr., A.B. Novaes, Clin. Oral Implants Res. 4 (1993) 106–110.
[261] A.J. Salgado, O.P. Coutinho, R.L. Reis, Macromol. Biosci. 4 (2004) 743–765.
[262] E. Roberts, L. Hardison, M. Brown, Production of Microbial Cellulose, European Patent No. 0186495, 1985.
[263] S. Yamanaka, E. Ono, K. Watanabe, M. Kusakabe, Y. Suzuki, Hollow Microbial Cellulose, Process for Preparation Thereof, and Artificial Blood Vessel Formed of Said Cellulose, European Patent EP0396344A2, 1990.
[264] D. Klemm, U. Udhardt, S. Marsch, D. Schumann, Method and Device for Producing Shaped Microbial Cellulose for Use as a Biomaterial, Especially for Microsurgery, US Patent No. US20030013163A1, 2001.
[265] D. Klemm et al., Prog. Polym. Sci. 26 (2001) 1561–1603.
[266] Y. Li et al., Adv. Healthc. Mater. 6 (2017) 1601343.
[267] X. Lv et al., ACS Biomater. Sci. Eng. 2 (2016) 19–29.
[268] M. Kołaczkowska et al., Mater. Sci. Eng. C 97 (2019) 302–312.
[269] W.K. Czaja et al., Biomacromolecules 8 (2007) 1–12.
[270] J. Wippermann et al., Eur. J. Vasc. Endovasc. Surg. 37 (2009) 592–596.
[271] H. Martínez Ávila et al., Biomaterials 44 (2015) 122–133.
[272] S.-H. Lee et al., J. Adv. Prosthodont. 7 (2015) 484.
[273] H. Zhang et al., Mater. Lett. 212 (2018) 118–121.
[274] L.R. Mello et al., J. Neurosurg. 86 (1997) 143–150.
[275] C.L. Rosen et al., Neurosurgery (2011) 1.
[276] E.S. Place, N.D. Evans, M.M. Stevens, Nat. Mater. 8 (2009) 457–470.
[277] H. and H.S. US Department, (2006).
[278] S. Shin, J. Hyun, ACS Appl. Mater. Interfaces 9 (2017) 26438–26446.
[279] G. Chinga-Carrasco, Biomacromolecules 19 (2018) 701–711.
[280] V.C.-F. Li et al., Sci. Rep. 7 (2017) 8018.
[281] R.E. Abouzeid et al., Biomacromolecules 19 (2018) 4442–4452.
[282] S.V. Murphy, A. Atala, Nat. Biotechnol. 32 (2014) 773–785.
[283] A. Sydney Gladman et al., Nat. Mater. 15 (2016) 413–418.
[284] M.K. Hausmann et al., ACS Nano 12 (2018) 6926–6937.
[285] H.P. Voisin et al., ACS Sustainable Chem. Eng. 6 (2018) 17160–17167.
[286] K.K. Moncal et al., Mater. Sci. Eng. C 105 (2019) 110128.
[287] S. Huan et al., Biomacromolecules 20 (2019) 635–644.
[288] R. Ajdary et al., Biomacromolecules 20 (2019) 2770–2778.
[289] V.C.F. Li et al., ACS Sustainable Chem. Eng. 6 (2018) 2011–2022.
[290] M. Müller et al., Ann. Biomed. Eng. 45 (2017) 210–223.
[291] L.G. Greca et al., Mater. Horizons 5 (2018) 408–415.
[292] A.M. Duraj-Thatte et al., Adv. Mater. 31 (2019) 1901826.
[293] M. Osorio et al., Mater. Sci. Eng. C 100 (2019) 697–705.
[294] C. Minas et al., Adv. Mater. 28 (2016) 9993–9999.
[295] S. Huan et al., Adv. Funct. Mater. 29 (2019) 1902990.
[296] S. Magdassi, O. Shoseyov, Colloids Interfaces 3 (2019) 1–15.
[297] T. Or et al., ACS Appl. Nano Mater. 2 (2019) 4169–4179.
[298] H.-J. Sung et al., Biomaterials 25 (2004) 5735–5742.
[299] K. Tomihata, Y. Ikada, Biomaterials 18 (1997) 567–575.
[300] L. Heath, L. Zhu, W. Thielemans, ChemSusChem 6 (2013) 537–544.